



HAL
open science

A membraneless starch/O₂ biofuel cell based on bacterial surface regulable displayed sequential enzymes of glucoamylase and glucose dehydrogenase

Yuanyuan Cai, Mingyang Wang, Shuqin Fan, Bo Liang, Xinxin Xiao, Zongmei Zheng, Serge Cosnier, Aihua Liu

► To cite this version:

Yuanyuan Cai, Mingyang Wang, Shuqin Fan, Bo Liang, Xinxin Xiao, et al.. A membraneless starch/O₂ biofuel cell based on bacterial surface regulable displayed sequential enzymes of glucoamylase and glucose dehydrogenase. *Biosensors and Bioelectronics*, 2022, 207, pp.114197. 10.1016/j.bios.2022.114197 . hal-03797632

HAL Id: hal-03797632

<https://hal.science/hal-03797632>

Submitted on 7 Oct 2022

HAL is a multi-disciplinary open access archive for the deposit and dissemination of scientific research documents, whether they are published or not. The documents may come from teaching and research institutions in France or abroad, or from public or private research centers.

L'archive ouverte pluridisciplinaire **HAL**, est destinée au dépôt et à la diffusion de documents scientifiques de niveau recherche, publiés ou non, émanant des établissements d'enseignement et de recherche français ou étrangers, des laboratoires publics ou privés.

A membraneless starch/O₂ biofuel cell based on bacterial surface regulable displayed sequential enzymes of glucoamylase and glucose dehydrogenase

Yuanyuan Cai, Mingyang Wang, Shuqin Fan^{1,a,b}, Bo Liang^{1,b}, Xinxin Xiao^{1, a,c}, Zongmei Zheng^a, Serge Cosnier^{d,e,*}, and Aihua Liu^{a,*}

^aInstitute for Biosensing, and College of Life Sciences, Qingdao University, Qingdao 266071, China

^bQingdao Institute of Bioenergy & Bioprocess Technology, Chinese Academy of Sciences, 189 Songling Road, Qingdao 266101, China

^cDepartment of Chemistry, Technical University of Denmark, 2800, Kongens Lyngby, Denmark

^dUniversity Grenoble Alpes DCM UMR 5250, F-38000 Grenoble, France

^eDépartement de Chimie Moléculaire, UMR CNRS, DCM UMR 5250, F-38000 Grenoble, France

¹Authors of equal contribution.

*Corresponding authors. E-mail addresses: liuah@qdu.edu.cn (A.L.); serge.cosnier@univ-grenoble-alpes.fr (S.C.)

Abstract

Enzymatic biofuel cells (EBFCs) provide a new strategy to enable direct biomass-to-electricity conversion, posing considerable demand on sequential enzymes. However, artificial blend of multi-enzyme systems often suffer biocatalytic inefficiency due to the rambling mixture of catalytic units. In an attempt to construct a high-performance starch/O₂ EBFC, herein we prepared a starch-oxidizing bioanode based on displaying a sequential enzyme system of glucoamylase (GA) and glucose dehydrogenase (GDH) on *E.coli* cell surfaces in a precise way using cohesin-dockerin interactions. The enzyme stoichiometry was optimized, with GA&GDH (3:1)-*E.coli* exhibiting the highest catalytic reaction rate. The bioanode employed polymerized methylene blue (polyMB) to collect electrons from the oxidation of NADH into NAD⁺, which jointly oxidized starch together with co-displayed GA and GDH. The bioanode was oxygen-insensitive, which can be combined with a laccase based biocathode, resulting in a membranless starch/O₂ EBFC in a non-compartmentalized configuration. The optimal EBFC exhibited an open-circuit voltage (OCV) of 0.74 V, a maximum power density of $30.1 \pm 2.8 \mu\text{W cm}^{-2}$, and good operational stability.

Keywords: Sequential enzymes; Bacterial surface display; Glucoamylase; Glucose dehydrogenase; Starch/O₂ biofuel cell.

1. Introduction

Polysaccharide based biomass represents a category of widely available and renewable natural resource (Zhao et al., 2017). Direct conversion of biomass into electricity, rather than burning, is a promising green energy technology largely relying on microbial fuel cells (MFCs), solid oxide fuel cells (SOFCs) and polymer-exchange membrane fuel cells (PEMFCs) (Liu et al., 2014). However, challenges remain for these fuel cells: namely the low power density of MFCs, high operation temperatures (generally over 500 °C) of SOFCs, and the sluggish catalytic activity of noble metal catalysts used in PEMFCs toward polysaccharide. Alternatively, enzymatic biofuel cells (EBFCs) are a subgroup of fuel cell utilizing enzymatic catalysts (Xiao et al., 2019). EBFCs can operate at mild temperature and neutral pH, making them potential power suppliers for portable or implanted devices using physiological mono-saccharides such as glucose and lactate as the fuel (Hou et al., 2014; Szczupak et al., 2012; Xiao et al., 2018a; Xiao et al., 2018b; Xiao et al., 2019). The energy density of EBFCs can be further improved using polysaccharide as the fuel, as polysaccharide possesses 11% higher energy density over glucose (Cheng et al., 2015). Further, the utilization of polysaccharide widens the scope of fuels for EBFCs (So et al., 2014; Zhu et al., 2014; Zhu et al., 2017).

Starch, a kind of polysaccharide made of glucose subunits linked with glycosidic bonds, exists widely in plants, which is an important feed and food source and a cost-effective substrate for the production of extensively industrial products (Lang et al., 2014). Previously, we developed a starch/O₂ EBFC based on a bioanode by the co-immobilization of commercially available glucoamylase (GA, EC 3.2.1.3) and glucose oxidase (GOx, EC 1.1.3.4) (Lang et al., 2014). In such a sequential-enzyme system, GA catalyzes the hydrolysis of starch into glucose units with the cleavage of the α -1, 4 and α -1, 6 glycosidic bonds at the non-reducing ends of starch. GOx can subsequently oxidize glucose into gluconolactone with two electrons involved, which can be collected by a solid electrode, i.e. the bioanode of an EBFC. In a similar approach, Yamamoto *et al.* assembled a membraneless white rice/O₂ EBFC using a carbon paste bioanode with GOx, alpha amylase and GA (Yamamoto et al., 2013). These cases adapt conventional single enzyme immobilization technology to immobilize multi-enzymes, aiming to combine the catalytic properties of different enzymes to

improve the efficiency of enzyme catalysis (Rodrigues et al., 2013). However, there are still many remaining challenges in the co-immobilization of enzymes (Wheeldon et al., 2016), including loss of enzyme activity, unsatisfactory compatibility of the vectors and tedious protein purification processes (Jia et al., 2014). Especially, random blend of multienzymes without precise control over spatial localization and orientation of enzyme typically constrains the overall catalytic efficiency.

Microbial surface display technology refers to the display of enzymes on the surface of microbial cells to form whole cell catalysts (Chen et al., 2011; Liang et al., 2013a; Liang et al., 2012; Liang et al., 2013b; Xia et al., 2013), owning the potential to immobilize multiple enzymes (Fujita et al., 2004). For example, Alfonta *et al.* displayed GA and GOx on the yeast surface respectively, leading to a two-chamber EBFC (Bahartan et al., 2012). However, the yielded maximum power density (P_{\max}) was not satisfying ($3 \mu\text{W cm}^{-2}$), which may be explained by the yeast cell induced steric hinderance and spatial barrier between two types of enzymes (Liang et al., 2013b).

Recently, we successfully co-displayed GA and GOx on yeast cell surface via cohesion-dockerin interaction with controllable and close localization of the sequential enzymes (Fan et al., 2020). This approach allows the tunable molecular ratio and preferred spatial orientation, enabling increased biocatalytic efficiency and optimizing overall pathway flux. The resulting starch/O₂ EBFC utilized a Nafion membrane to construct a two-chamber setup (Fan et al., 2020), as O₂ could inevitably react with GOx to form H₂O₂ that is harmful to the biocathode enzyme (Milton et al., 2014). It will greatly simplify the configuration and reduce the cost of the EBFC to eliminate the Nafion membrane, which can be achieved by using O₂ insensitive NAD⁺ (the oxidized form of nicotinamide adenine dinucleotide) dependent glucose dehydrogenase (GDH, EC 1.1.1.47), with the resultant NADH (the reduced form of NAD⁺) oxidized on the bioanode. In this contribution to construct membraneless EBFCs, we prepared a bioanode with a sequential enzyme system of GA/GDH co-displayed on the bacteria surface (GA&GDH (n:1, n=1,2,3,4)-*E.coli*) in a controllable manner. Coupled with a *Trametes versicolor* laccase biocathode undergoing direct electron transfer (DET), the co-displayed GA&GDH-*E.coli* bioanode based EBFCs outperformed the randomly mixed system regarding to power density and operational stability. In terms of the effect of molecular ratio,

the EBFC using a GA&GDH (3:1)-*E.coli* bioanode presented the highest open-circuit voltage of about 0.74V and the largest P_{\max} of $30.1 \pm 2.8 \mu\text{W cm}^{-2}$ as well as good operational stability.

2. Experimental section

2.1 Reagents

NAD⁺ was purchased from Blue Season Biotechnology Company (Shanghai, China). *Trametes versicolor* laccase (*TvLc*) with a specific activity of 13.6 U mg⁻¹ was purchased from Sigma-Aldrich (St. Louis, MO, USA), which was purified before use by a dialysis-membrane with a 10 000-MW cut-off. The specific activity of purified *TvLc* was assayed to be 18.3 U mg⁻¹. Multiwalled carbon nanotubes (MWCNTs) with a length of less than 2 μm and a diameter 10-20 nm were purchased from Shenzhen Nanoport Co. Ltd (Shenzhen, China). Starch, maltose, glucose, methylene blue (MB) and chitosan were bought from Sinopharm Chemicals Co., Ltd (Shanghai, China).

2.2 Bacterial cell surface display

Briefly, chimeric scaffoldins containing cohesins on the *E.coli* surface were first prepared. *E. coli* cells harboring pTInaPbN-cohC-cohT, pTInaPbN-cohC-cohT-cohC, pTInaPbN-cohC-cohT-cohC-cohC and pTInaPbN-cohC-cohT-cohC-cohC-cohC were cultured in a LB medium. Dockerin-fused GA (GA-DocC) and GDH (DocT-GDH) were then expressed in *E. coli* BL21 (DE3) and assembled on the surfaces of the bacteria cells with displayed scaffoldins, due to the high specificity of cohesin-dockerin interaction.

The overall reaction of GA-GDH combination was conducted at 40 °C for 15 min in phosphate buffer (PB, 50 mM, pH 6.0) containing NAD⁺ (3 mM) and maltose (30 mM). The overall reaction rate is defined as the amount of liberated NADH per min using per entire OD₆₀₀ cells under assay conditions.

Additionally, the assembly route of GA-DocC and DocT-GDH loading onto the chimeric scaffolds can influence the corresponding catalytic efficiency. The superior performance could be achieved when DocT-GDH was loaded onto the scaffold prior to GA-DocC in a step-by-step way, due to the mismatch of the optimal working pH 5-6 for GA (Zheng et al., 2010) and pH 4.5-10.5 for GDH (Liang et al., 2013a). When GA-DocC was first loaded onto

chimeric scaffoldin prior to DocT-GDH, GA cannot stand the pH 8.0 buffer for the subsequent DocT-GDH assembly.

The number ratios of GA-DocC to DocT-GDH were approximately 1:1, 2:1, 3:1 and 4:1, when CohC-CohT, CohC-CohT-CohC, CohC-CohT-CohC-CohC and CohC-CohT-CohC-CohC-CohC were separately displayed on the surface of cell, consistent with the original design of enzymes co-display systems with controllable ratio (Table S1).

2.3 Preparation of modified bioanode and biocathode

A 4 μL aliquot of 2 mg mL^{-1} MWCNTs dispersion in N, N-dimethylformamide was drop-cast on a well-polished glassy carbon electrode (GCE, diameter: 3 mm), allowing to dry in air to acquire MWCNTs/GCE. The as-prepared MWCNTs/GCE was immersed in a 0.2 mM MB aqueous solution for 3 h to adsorb the monomer, followed by soaking in water for 5 min to remove any loosely bound MB molecules. The adsorbed MB was electropolymerized in 0.2 M pH 6.0 PB for 60 min at a constant potential of 0.85 V vs. SCE to obtain polyMB-MWCNTs/GCE (Yan et al., 2006). A 3 μL aliquot of GA&GDH (n:1)-*E.coli* (n: 1, 2, 3 and 4) aqueous dispersion was carefully placed onto the modified GCE, which was dried overnight at 4 °C. Finally, 5 μL chitosan solution (0.05 w/v) was coated onto the electrode surface. The as-prepared bioanodes were denoted as GA&GDH (n:1)-*E.coli*/polyMB-MWCNTs/GCE. Control electrodes with either GA-*E.coli* or GDH-*E.coli* were also prepared with the same procedure.

For the preparation of TvLc/MWCNTs based biocathodes, an established procedure reported previously by our group was followed (Hou et al., 2017).

2.4 Assembly of biofuel cell

The starch/O₂ EBFC was assembled by immersing the prepared bioanode and biocathode into a 5 mL electrochemical cell. The EBFC performance was tested in oxygen-saturated 0.2 M pH 5.0 McIlvaine buffer containing 4 mM NAD⁺ with various starch concentrations. No Nafion membranes were used herein.

2.5 Electrochemical studies

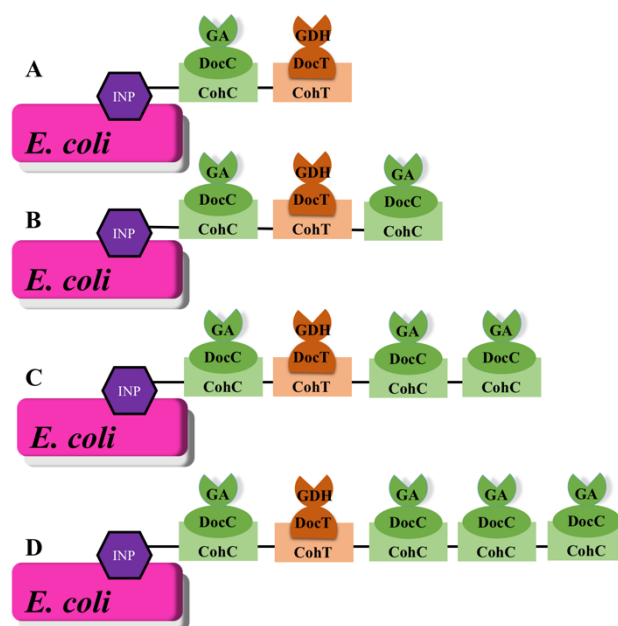
Electrochemical studies were carried out with a CHI 660E potentiostat (Shanghai, China).

The modified bioelectrodes were electrochemically characterized and used as the working electrode in a conventional three-electrode system with a Pt wire auxiliary electrode and a saturated calomel electrode (SCE) reference electrode.

3. Results and discussion

3.1 Controllable construction of bacteria surface display systems

Sequential enzyme-displaying system in a ratio- and position- controllable manner was successfully constructed (Scheme 1). This is because that chimeric scaffold proteins containing CohC-CohT, CohC-CohT-CohC, CohC-CohT-CohC-CohC and CohC-CohT-CohC-CohC-CohC were separately displayed on the cell surface of *E. coli* using ice nucleation protein (INP) as an anchoring motif. Dockerin-fused-GDH and dockerin-fused-GA were successfully expressed onto *E. coli* showing considerable enzymatic activities, with a biological activity of 4.34 ± 0.05 and 2.53 ± 0.08 U mg^{-1} , respectively, implying that enzymes were in favorable conformation. Unifunctional systems were constructed by loading the saturated volumes of crude enzyme extracts containing GA-DocC or DocT-GDH onto the cells based on cohesin-dockerin interaction. The cascade reaction catalyzed by the GA/GDH pair is limited by the hydrolysis of substrate by GA due to the lower affinity and kinetics when compared to the glucose oxidation catalyzed by GDH (Baik et al., 2005; Zheng et al., 2010). It is hypothesized that the overall reaction rate could be enhanced by compensating GA amount to guarantee sufficient proximate glucose concentration for GDH. NADH production rate was measured to reflect the speed of starch degradation and increased with GA/GDH ratio from 1:1 to 3:1. GA&GDH (3:1)-*E. coli* showed the highest level of NADH production rate (41.97 ± 1.95 nmol min^{-1}) over other ratios and other multi-enzyme systems with the same ratio (Figure S1). However, the overall reaction rate (35.31 ± 1.73 nmol min^{-1}) decreased when the ratio 4:1, probably due to that large passenger protein (the molecular weight of INP-CohC-CohT-CohC-CohC-CohC protein is about 120 kDa) hindered the expression efficiency and surface display (Fan et al., 2012).



Scheme 1. The schematic representation for the co-display of sequential enzymes on the bacteria surface through bifunctional scaffoldins. Enzyme molecular ratios of GA to GDH are 1:1 (A), 2:1 (B), 3:1 (C) and 4:1 (D), separately.

3.2 Electrochemical characterization of the bioanode

The co-displayed enzyme system served as anodic biocatalyst for starch oxidation was investigated. As depicted in eq. S1, starch is first hydrolyzed into glucose by the catalysis of GA, which is subsequently oxidized by GDH in the presence of NAD^+ , resulting in NADH. NADH can be electrochemically oxidized on the electrode shuttling electrons to the electrode surface, *i.e.* the basis for electrochemical biosensors and bioanode utilizing NAD^+ as the cofactor (Liu et al., 2006). Cyclic voltammograms (CVs) of a bare GCE in the buffer solution containing NAD^+ and GA&GDH (1:1)-*E.coli* without any substrates (Figure S2) showed silent redox peaks. In the presence of 0.1% (w/v) starch or 4 mM glucose, sigmoidal curves turned to appear implying the oxidation of substrates with an onset potential of 0.2 V vs. SCE (Figure S2). It is noteworthy that the co-enzyme system could also oxidize disaccharide maltose (4 mM, Figure S2), with an oxidation current higher than that of starch, but lower than glucose. This confirms that the cascade reaction was limited by the catalytic hydrolysis of polysaccharide with GA.

To decrease the overpotential of NADH oxidation and increase catalytic current density,

electropolymerized methylene blue (polyMB) on MWCNTs modified electrodes was utilized for the immobilization of microbial surface displayed enzyme (Figure S3). The electropolymerization process was performed at a constant potential at +0.85 V vs. SCE. The formation of MB-MWCNTs adduct was investigated by CV at different intervals. In consistence with previous reports (Wen et al., 2010; Yan et al., 2006), the peak currents at -0.22 V vs. SCE obtained for the MB-MWCNTs adduct decreased with time (Figure S2), and a pair of new redox peaks at -0.09 V appeared, with the peak currents increasing with the time, proving the formation of the polyMB-MWCNTs composite.

The oxidation of starch at the GA&GDH (n:1, n=1, 2, 3, 4)-*E.coli*/polyMB-MWCNTs bioanodes presented an onset potential of ca. -0.04 V (Figure 1A-D), much lower than that at the bare GCE (0.2 V, Figure S2) and comparable to that of polyMB/single-walled CNTs (Wen et al., 2010). The background-corrected oxidation current density (Δj_a) varied with enzyme molecule ratio of GA to GDH displayed onto the strain (Figure 1E). Δj_a increased with the GA amount as the displayed GA&GDH ratio increased from 1:1 to 2:1 and to 3:1, however, it leveled off when the ratio increased to 4:1 (Figure 1E). Such a trend is consistent to the observation with the observed biocatalysis results (Figure S1). GA&GDH (3:1)-*E.coli* based bioelectrode (Figure 1C) registered a Δj_a of $27.0 \pm 1.9 \mu\text{A cm}^{-2}$, which was 2.5-fold of that value of GA&GDH (1:1)-*E.coli* based bioelectrode ($10.6 \pm 1.3 \mu\text{A cm}^{-2}$, Figure 1A). The enhanced Δj_a validated the effort on adjusting enzyme stoichiometry of GA/GDH is paid off. The further increased oxidation signal with mass concentrations of starch further verified the successful catalytic reaction on the GA&GDH (3:1)-*E.coli* based bioelectrode (Figure 1F).

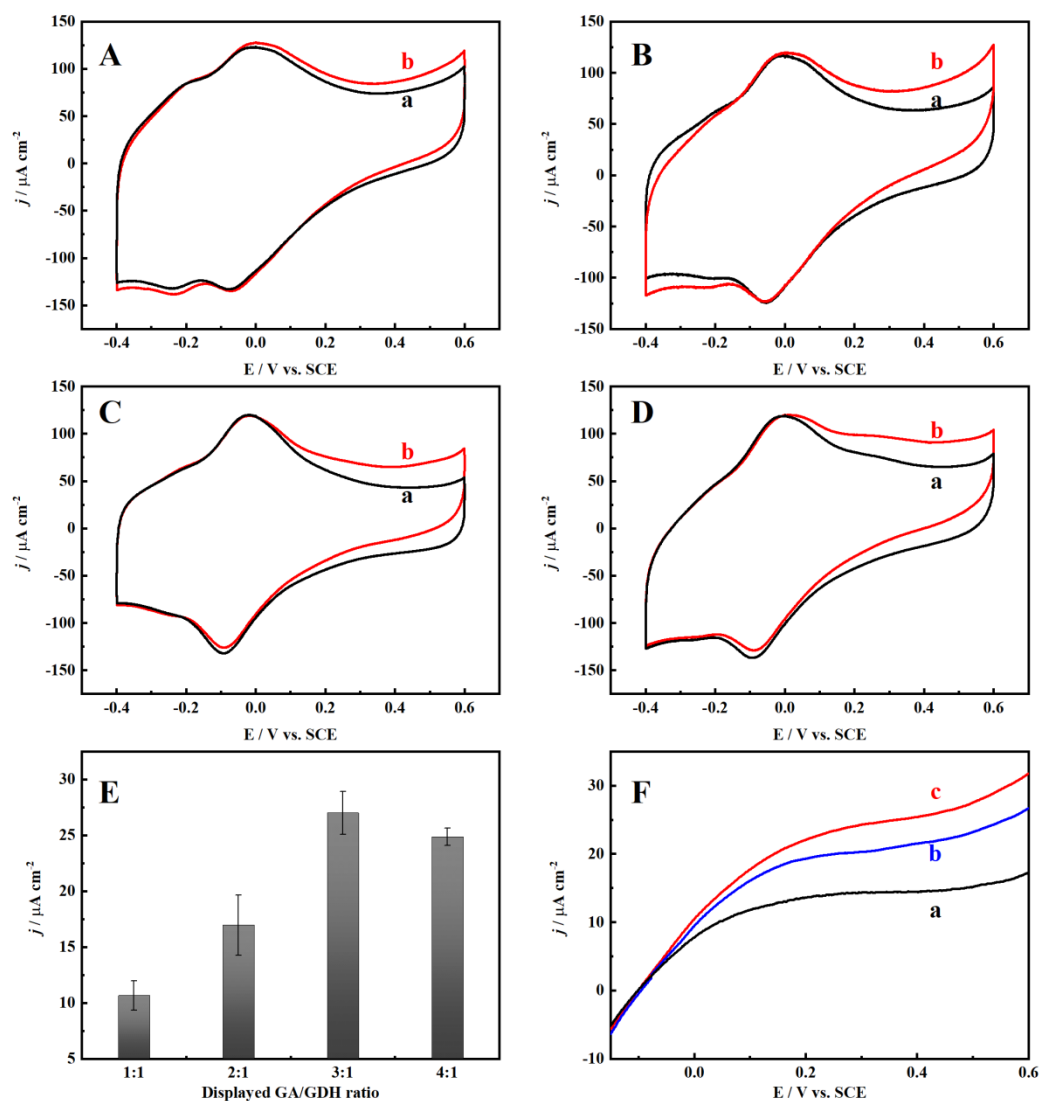


Figure 1. (A-D) CVs of the GA&GDH(n:1)-*E.coli*/polyMB-MWCNTs/GCE in 0.2 M pH 5.0 McIlvaine buffer (phosphate-citric acid buffer) containing 4 mM NAD⁺ in the absence (a) and presence of 1.0% (w/v) starch (b). n=1 (A), 2 (B), 3 (C), 4 (D). Scan rate: 20 mV s⁻¹. (E) The dependency of Δj_a at 0.3 V on the enzyme molecule ratio of GA to GDH displayed onto the strain. (F) Polarization curves of the GA&GDH(3:1)-*E.coli*/polyMB-MWCNTs/GCE in 0.2 M pH 5.0 McIlvaine buffer containing 4 mM NAD⁺ with different starch concentrations: 0.5% (w/v) (a), 1.0% (w/v) (b) and 2.0% (w/v) starch (c). Scan rate: 1 mV s⁻¹.

3.3 Characterization of the starch/O₂ EBFCs

One-compartment starch/O₂ EBFCs consisting of *TvLc*/MWCNTs/GCE biocathodes (Hou et al., 2017) and GA&GDH (n:1, n=1, 2, 3, 4)-*E.coli*/poly MB-MWCNTs/GCE bioanodes were assembled (Figure 2A). The dependence of power density on enzyme

molecule ratio of GA to GDH showed a similar trend (Figure 2B) as observed for biocatalysis results (Figure S1), because the overall EBFCs were limited by the bioanodes with much lower current density than that of the *TvLc* based cathode. The EBFC with a GA&GDH (3:1)-*E.coli* bioanode exhibited a maximum output power density (P_{\max}) of $30.2 \pm 2.8 \mu\text{W cm}^{-2}$ at 0.46 V and an open-circuit voltage (OCV) of 0.74 V (Figure 2B, curve c). The optimal P_{\max} achieved when $n=3$ outperformed the other ratios (14.1 ± 1.7 , 24.4 ± 2.1 and $27.8 \pm 2.3 \mu\text{W cm}^{-2}$ for $n=1, 2$ and 4 , respectively), also comparable to our previous work utilizing co-displayed GA&GOx on the yeast cell surface (36.1 ± 2.5) (Fan et al., 2020).

To verify the critical roles of co-display and surface display, GA-*E.coli* & GDH-*E.coli* (3:1)/polyMB-MWCNTs/GCE (b) and free-GA & free-GDH (3:1)/polyMB-MWCNTs/GCE were also prepared with same enzyme amounts (in activity) as that on GA&GDH (3:1)-*E.coli*/polyMB-MWCNTs/GCE. Starch/ O_2 EBFCs using those bioanodes (22.3 ± 2.5 and $18.7 \pm 1.6 \mu\text{W cm}^{-2}$ for non-co-display and non-surface-display, respectively, Figure 3) registered inferior P_{\max} to that of GA&GDH (3:1)-*E.coli* bioanode-based EBFC ($30.2 \pm 2.8 \mu\text{W cm}^{-2}$), highlighting the importance of enzyme localization in a sequential enzyme system. The co-displayed system is likely to promote the tunneling of intermediate in proximity between GA and GDH that are bound to the same scaffoldin. Further, the co-display, separate-display and free enzyme systems with a ratio of GA&GDH (3:1) showed a higher than that of co-displayed GA&GDH (1:1)-*E.coli* ($14.1 \pm 1.7 \mu\text{W cm}^{-2}$). It could be conclusive that enzyme stoichiometry is also the governing factor, confirming again the hydrolysis of starch is the rate-determining step in such a cascade reaction.

In previous studies, co-immobilized GA and GOx for starch/oxygen EBFC showed a P_{\max} of $8.15 \mu\text{W cm}^{-2}$ and an OCV of 0.53V (Lang et al., 2014), a microbial BFC with GA-displaying yeast and GOx-displaying yeast as the anodic catalysts showed a P_{\max} of $1.8 \mu\text{W cm}^{-2}$ and an OCV of 0.63V (Bahartan et al., 2012). Such low performance may be attributed to the negative influence of uncontrollable ratio and uncertain spatial organization of enzymes on substrate diffusion during each step of enzymatic reactions (Dueber et al., 2009; Kim et al., 2010). In comparison, the microbial cell surface co-displayed sequential-enzyme (including GA&GDH-*E.coli* in this work and our previous GA&GOx-yeast (Fan et al., 2020)) based starch/ O_2 EBFCs exhibited the highest OCV and P_{\max} . The enhanced cascade reaction rate and

the corresponding starch/O₂ EBFC can be attributed to that the precisely tailored ratio and suitable spatial organization of *E.coli* surface displayed GA and GDH.

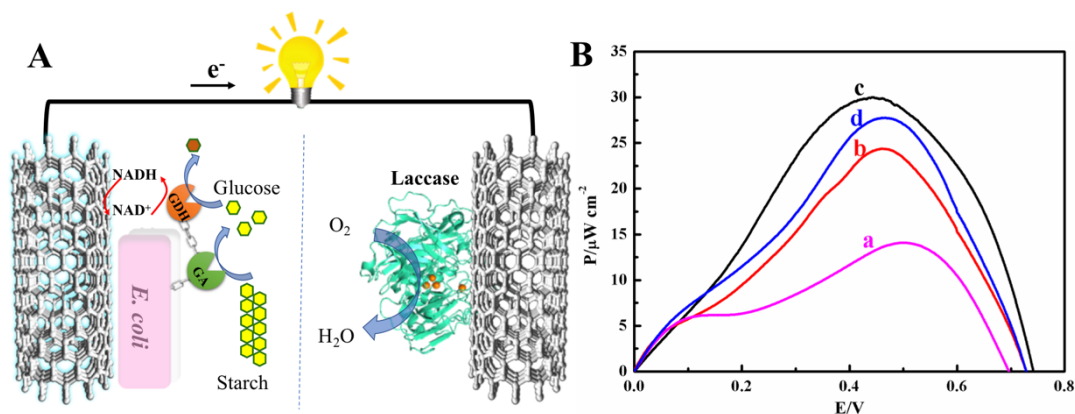


Figure 2. (A) Schematic drawing of the assembled EBFC. (B) Power density profiles of starch/O₂ EBFCs using GA&GDH (n:1)-*E.coli*/polyMB-MWCNTs/GCE, n=1 (a), n=2 (b), n=3 (c) and n=4 (d) as bioanodes. Solution: O₂ saturated 0.2 M pH 5.0 McIlvaine buffer containing 4 mM NAD⁺ and 1.0% (w/v) starch.

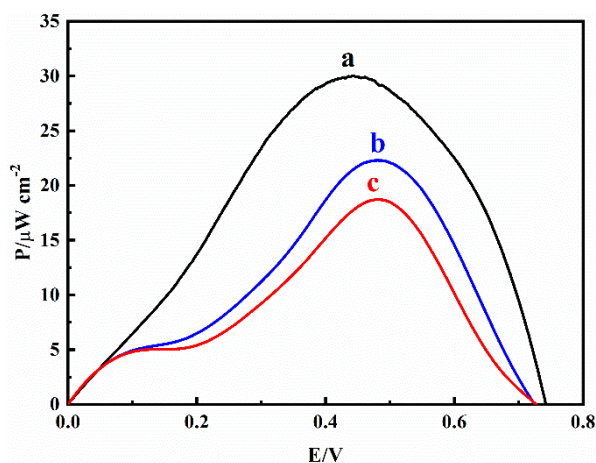


Figure 3. Power density profiles of starch/O₂ EBFCs using GA&GDH (3:1)-*E.coli*/polyMB-MWCNTs/GCE (a), GA-*E.coli* & GDH-*E.coli* (3:1)/polyMB-MWCNTs/GCE (b) and free-GA & free-GDH (3:1)/polyMB-MWCNTs/GCE (c) bioanodes. Solution: O₂ saturated 0.2 M pH 5.0 McIlvaine buffer containing 4 mM NAD⁺ and 1.0% (w/v) starch.

Operational stability is another important criterion of EBFC (Xiao et al., 2019). In a course of 8 h continuous operation (Figure 4), 85% of original P_{\max} was retained for GA&GDH (3:1)-*E.coli* based EBFC, much better than those for a GA-*E.coli* & GDH-*E.coli* (72%) and a free GA & free GDH bioanode (69%) based EBFC. These results indicate a favorably stable power output process, probably benefited from appropriate ratio and ordering of enzymes co-

displayed on biocompatible *E. coli* surface (Fan et al., 2020; Liang et al., 2012).

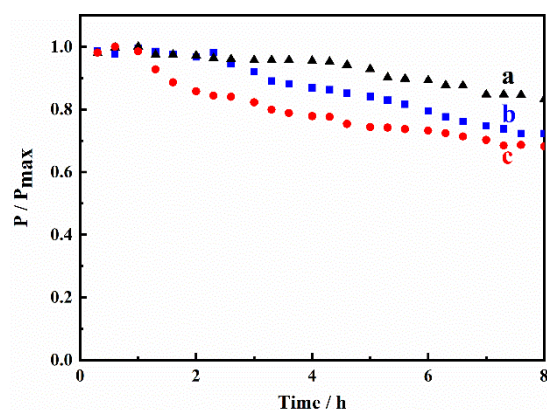


Figure 4. The operational stabilities of EBFCs with different enzymes based bioanodes: GA&GDH (3:1)-*E. coli* (a), GA-*E. coli* & GDH-*E. coli* (b) and free GA & free GDH (c). P is the power measured as a function of time, and P_{\max} is the initial maximum power density.

4. Conclusions

Direct biomass-to-electricity conversion has been successfully demonstrated by preparing membrane-less starch/O₂ EBFCs consisting of GA&GDH (n:1, n=1, 2, 3, 4)- *E. coli*/polyMB-MWCNTs/GCE bioanodes and *TvLc*/MWCNTs/GCE biocathodes. The bioanode is oxygen-insensitive. The ratio of GA/GDH has been optimized, as hydrolysis of starch has been identified as the rate-determining step in such a sequential reaction for starch oxidation. Co-display of GA&GDH on *E. coli* cell surfaces also enhances the power density and operational stability, due to the precisely tailored enzyme localization and biocompatible microenvironment. The present work provides guidelines on adjusting enzyme stoichiometry and localization for superior performance with sequential enzyme cell surface display system. Future efforts such as improving the intrinsic activity of glucoamylase will be paramount.

CRedit authorship contribution statement

Shuqin Fan: Methodology, Investigation and Writing - Original Draft. **Bo Liang:** Investigation and Writing - Original Draft. **Xinxin Xiao:** Investigation and Writing - Original Draft. **Zongmei Zheng:** Investigation. **Serge Cosnier:** Writing - Review & Editing. **Aihua Liu:** Funding acquisition, Supervision, Conceptualization and Writing - Review & Editing.

Acknowledgments

This work was financially supported partially by the National Key Research and Development

Program of China (2021YFA0910400) and National Natural Science Foundation of China (81673172).

References

- Bahartan, K., Amir, L., Israel, A., Lichtenstein, R.G., Alfonta, L., 2012. *ChemSusChem* 5(9), 1820-1825.
- Baik, S.-H., Michel, F., Aghajari, N., Haser, R., Harayama, S., 2005. *Appl. Environ. Microbiol.* 71(6), 3285-3293.
- Chen, I., Dorr, B.M., Liu, D.R., 2011. *Proc. Natl. Acad. Sci.* 108(28), 11399-11404.
- Cheng, K., Zhang, F., Sun, F., Chen, H., Percival Zhang, Y.H., 2015. *Sci. Rep.* 5(1), 13184.
- Dueber, J.E., Wu, G.C., Malmirchegini, G.R., Moon, T.S., Petzold, C.J., Ullal, A.V., Prather, K.L.J., Keasling, J.D., 2009. *Nat. Biotechnol.* 27(8), 753-759.
- Fan, L.H., Zhang, Z.J., Yu, X.Y., Xue, Y.X., Tan, T.W., 2012. *Proc. Natl. Acad. Sci.* 109(33), 13260-13265.
- Fan, S., Liang, B., Xiao, X., Bai, L., Tang, X., Lojou, E., Cosnier, S., Liu, A., 2020. *J. Am. Chem. Soc.* 142(6), 3222-3230.
- Fujita, Y., Ito, J., Ueda, M., Fukuda, H., Kondo, A., 2004. *Appl. Environ. Microbiol.* 70(2), 1207-1212.
- Hou, C., Liu, A., 2017. *Electrochim. Acta* 245(Supplement C), 303-308.
- Hou, C., Yang, D., Liang, B., Liu, A., 2014. *Anal. Chem.* 86(12), 6057-6063.
- Jia, F., Narasimhan, B., Mallapragada, S., 2014. *Biosens. Bioelectron.* 111(2), 209-222.
- Kim, D.C., Sohn, J.I., Zhou, D., Duke, T.A.J., Kang, D.J., 2010. *ACS Nano* 4(3), 1580-1586.
- Lang, Q., Yin, L., Shi, J., Li, L., Xia, L., Liu, A., 2014. *Biosens. Bioelectron.* 51(0), 158-163.
- Liang, B., Lang, Q., Tang, X., Liu, A., 2013a. *Bioresour. Technol.* 147(0), 492-498.
- Liang, B., Li, L., Mascin, M., Liu, A., 2012. *Anal. Chem.* 84(1), 275-282.
- Liang, B., Li, L., Tang, X., Lang, Q., Wang, H., Li, F., Shi, J., Shen, W., Palchetti, I., Mascini, M., Liu, A., 2013b. *Biosens. Bioelectron.* 45, 19-24.
- Liu, A., Watanabe, T., Honma, I., Wang, J., Zhou, H., 2006. *Biosens. Bioelectron.* 22(5), 694-699.
- Liu, W., Mu, W., Liu, M., Zhang, X., Cai, H., Deng, Y., 2014. *Nat. Commun.* 5, 3208.
- Milton, R.D., Giroud, F., Thumser, A.E., Minter, S.D., Slade, R.C.T., 2014. *Chem. Commun.* 50(1), 94-96.
- Rodrigues, R.C., Ortiz, C., Berenguer-Murcia, A., Torres, R., Fernandez-Lafuente, R., 2013. *Chem. Soc. Rev.* 42(15), 6290-6307.
- So, K., Kawai, S., Hamano, Y., Kitazumi, Y., Shirai, O., Hibi, M., Ogawa, J., Kano, K., 2014. *Phys. Chem. Chem. Phys.* 16(10), 4823-4829.
- Szczupak, A., Halamek, J., Halamkova, L., Bocharova, V., Alfonta, L., Katz, E., 2012. *Energy Environ. Sci.* 5(10), 8891-8895.
- Wen, D., Deng, L., Zhou, M., Guo, S.J., Shang, L., Xu, G.B., Dong, S.J., 2010. *Biosens. Bioelectron.* 25(6), 1544-1547.
- Wheeldon, I., Minter, S.D., Banta, S., Barton, S.C., Atanassov, P., Sigman, M., 2016. *Nat. Chem.* 8(4), 299-309.
- Xia, L., Liang, B., Li, L., Tang, X., Palchetti, I., Mascini, M., Liu, A., 2013. *Biosens. Bioelectron.* 44(0), 160-163.
- Xiao, X., Magner, E., 2018a. *Chem. Commun.* 54(46), 5823-5826.
- Xiao, X., Siepenkoetter, T., Conghaile, P.Ó., Leech, D., Magner, E., 2018b. *ACS Appl. Mater. Interfaces*

10(8), 7107-7116.

Xiao, X., Xia, H.-q., Wu, R., Bai, L., Yan, L., Magner, E., Cosnier, S., Lojou, E., Zhu, Z., Liu, A., 2019. *Chem. Rev.* 119(16), 9509-9558.

Yamamoto, K., Matsumoto, T., Shimada, S., Tanaka, T., Kondo, A., 2013. *New Biotechnol.* 30(5), 531-535.

Yan, Y., Zheng, W., Su, L., Mao, L., 2006. *Adv. Mater.* 18(19), 2639-2643.

Zhao, X., Liu, W., Deng, Y., Zhu, J.Y., 2017. *Renew. Sustain. Energy Rev.* 71, 268-282.

Zheng, Y.Y., Xue, Y.F., Zhang, Y.L., Zhou, C., Schwaneberg, U., Ma, Y.H., 2010. *Appl. Microbiol. Biotechnol.* 87(1), 225-233.

Zhu, Z., Kin Tam, T., Sun, F., You, C., Percival Zhang, Y.H., 2014. *Nat. Commun.* 5, 3026.

Zhu, Z., Zhang, Y.H.P., 2017. *Metab. Eng.* 39, 110-116.